Passive thermal behaviour of buildings: performance of external multi-layered walls and influence of internal walls

Francesco Leccese[1], Giacomo Salvadori[1], Francesco Asdrubali[2], Paola Gori[2]

[1] University of Pisa, School of Engineering, Largo Lucio Lazzarino, 56122 Pisa (Italy)
[2] Roma Tre University, Department of Engineering, Via della Vasca Navale 79, 00146 Roma (Italy)

Abstract
In contemporary architecture, the opaque building envelope is usually realised by multi-layered walls; that is, a sequence of homogeneous layers of different materials. The layer sequence and distribution affect the wall behaviour in terms of its overall thermal inertia, or heat storage capability; hence, analysis of the thermal performance of a multi-layered wall becomes very important under dynamic heat transfer conditions, as usually occurs during summer.
In this study, the authors employ analytical models based on the heat transfer matrix method, with the aim of predicting the dynamic thermal behaviour of external and internal building walls. Although numerous studies have been devoted to investigating the dynamic thermal behaviour of walls, the approach followed and results obtained by the authors are original and have significant implications that are of practical interest. By using the analytical models, the effects of continuous variations in the positioning and thickness distribution of the insulation material on the dynamic thermal performance (dynamic thermal transmittance, decrement factor and time lag) are demonstrated with reference to different constructive solutions (from a light-weight wall with a surface mass of 85 kg/m^2 to a massive wall with a surface mass of 294 kg/m^2). Moreover, a simplified correlation is proposed, which allows for correction of the dynamic thermal transmittance and time lag of external walls to take consider the effect of the internal walls (partition walls and slabs) on the dynamic thermal behaviour of a room. The results presented in the paper can be used during the building envelope design stage as a guideline for the improvement of the dynamic thermal performance of multi-layered walls. Furthermore, the insight provided into the building envelope thermal behaviour could prove useful for understanding how to maximise the effectiveness of possible retrofit interventions.

Keywords
Building envelope; Multi-layered walls; Internal walls; Dynamic thermal behaviour; Decrement factor; Time lag

Nomenclature
c, specific heat capacity, J/kgK;
C, surface thermal capacity, J/m^{2}K;
d, D, thickness, m;
E, thermal effusivity, Ws$^{1/2}$/m^{2}K;
f_a, decrement factor, defined in Eq.(5), dimensionless;
j, j=(−1)$^{1/2}$;
ℓ, admittance, W/m^{2}K;
M_S, surface mass, kg/m^2;
P, period, s;
q, Q, thermal power, W/m^2;
R, thermal resistance, m^{2}K/W;
S, surface, m^2;
t, time, s;
T, temperature, K;

U, thermal transmittance, W/m^2K;
V, volume, m^3;
z_{11}, z_{12}, z_{21}, z_{22}, elements of heat transfer matrix of internal walls;
Z_{11}, Z_{12}, Z_{21}, Z_{22}, elements of heat transfer matrix of external wall;
Z, heat transfer matrix of external wall;
Y_{ie}, dynamic thermal transmittance, defined in Eq.(5), W/m^2K.

Greek symbols
α, thermal diffusivity ($=\lambda/\rho c$), m^2/s;
γ, dimensionless parameter, defined in Eq.(A3);
ζ, dimensionless parameter, defined in Eq.(13);
η, fraction of thermal insulation placed on internal side of concrete;
λ, thermal conductivity, W/mK;
Λ, total admittance, defined in Eq.(12);
μ, dimensionless parameter, defined in Eq.(14);
ν, weight of k-th internal wall;
ξ, fraction of concrete externally disposed with respect to thermal insulation;
ρ, density, kg/m^3;
φ, time lag, defined in Eq.(5), s;
ψ, time lag, defined in Eq.(14), s;
ω, angular frequency, rad/s.

Subscripts
C, concrete;
e, external;
k, k-th internal wall;
i, internal;
lim, limit value;
n, n-th homogeneous layer.

1- Introduction

Buildings are responsible of a large share of total energy uses and CO_2 emissions. In Europe, in particular, the construction sector accounts for 40% of energy requirements and 36% of CO_2 emissions [1]. Provided that careful design strategies be employed, the building sector can be also identified as a source of significant possible energy savings, as approximately 75% of buildings are rated as energy inefficient [2].
One of the simplest and most effective ways of pursuing energy savings in buildings is by acting on their envelope, which represents the path for large amounts of heat flows. The thermal performance of the opaque building envelope plays such an important role in reducing building energy consumption that several studies were devoted to the evaluation of the influence of walls (especially external) thermal behaviour on building's energy consumption and on their energy saving potential [3-6]. As a rule, the external walls of buildings are multi-layered; that is, forming a sequence of homogeneous layers of different materials, some of which are endowed with resistive thermal properties (e.g. light and insulating layers), and others with capacitive thermal properties (e.g. heavy layers provided with mechanical resistance).
Under steady state conditions, the thermal behaviour of a multi-layered wall is defined by its thermal transmittance, the value of which is independent of the layer sequence. Dependence on the layer sequence order is obviously exhibited by the temperature variation inside the wall and,

consequently, by the interstitial hygrometric behaviour. This, in turn, may affect the wall dynamic behaviour, as its thermo-physical properties are modified by the moisture content [7].
However, most importantly, the layer sequence and distribution affect the wall behaviour in terms of its overall thermal inertia, namely, its heat storage capability. A large amount of studies has been devoted to investigating this issue [8]. The so-called 'thermal flywheel effect', consisting of the reduction and phasing out of temperature fluctuations achieved inside a building when using massive walls, has been studied since the 80s. Duffin and Knowles [9,10] optimised this effect by acting on the design of a multi-layered wall. Tsilingiris [11] studied the same effect by analysing the dynamic behaviour of increasingly heavier walls in terms of their ability to damp out and phase out internal heat flux. In another study, the same author [12] further investigated the combined distribution effects of heat capacity and thermal resistance in many different multi-layered wall types, highlighting the fact that the building envelope effective heat capacity is strongly affected by the distribution of resistive and capacitive layers.
The concepts of decrement factor and time lag were employed extensively to compare alternatives quantitatively by Asan [13,14]. The decrement factor is defined as the ratio between internal and external surface temperature oscillations, while the time lag identifies the delay between the occurrence of an external surface temperature event and its corresponding manifestation on the internal surface. By numerically solving the one-dimensional heat conduction equation using a Crank-Nicholson scheme and convection boundary conditions, Asan analysed several different multi-layered wall configurations by changing the insulation layer position and thickness.
Kossecka and Kosny [15] analysed the manner in which heating and cooling loads are affected by the wall configuration. They introduced a thermal structure factor that considers the spatial distribution of thermal resistance and capacity within the wall. The result was that performance is improved by concentrating the massive layers towards the internal environment, with an additional dependence on the climate type.
Al-Sanea et al. [16] used a finite-volume model based on numerical integration of the one-dimensional heat conduction equation in order to determine the optimum thickness of an insulation layer under Riyadh climate conditions. This was subsequently used to analyse the effects of different locations and distributions of the insulation layer. Optimal performance was obtained with three insulation layers, placed from the outside, from the inside and in the middle of the wall, respectively. In other studies by the same research group, the thermal mass amount and location were optimised [17], and the effects of the type of masonry material and surface absorptivity to solar radiation were analysed [18].
Significant contributions were also provided by Ozel and Pihtili [19]. By means of the numerical finite-difference solution of the one-dimensional heat conduction equation, these authors studied the effect of differently locating an insulation layer within a multi-layered wall in the climatic conditions of Elazığ, Turkey, also considering the influence of wall orientation. In their work, the distribution of insulation layers with three placements (from the outside, from the inside and in the middle) was found to provide optimal results. Furthermore, the optimum insulation thickness was determined using the same method in [20], and it was found that yearly transmission loads, and therefore also optimum insulation thickness, are not affected by insulation location, which agrees with the outcomes of other works [16].
Thermal insulation improvement was the aim of the work by Bond et al. [21]: an electrical analogy was used to describe one-dimensional heat conduction and compare several walls, where only the layer distribution was varied, in terms of their decrement factor and time lag. With the same objective of maximising insulation, Gori et al. [22] used a heat transfer matrix approach to derive a basic inequality on the effect produced by layer order on the decrement factor, and to study the effects of layer location and distribution on wall performance. Zhang et al. analysed how wall configuration affects heating and cooling loads in five climatic zones in China, also determining optimum insulation thickness by life cycle cost analysis [23].

Alternative retrofit solutions for Greek buildings, involving the application of an insulation layer from the outside or inside, were compared by Kolaitis et al. [24]. It was revealed that insulation from the outside is more advantageous than that from the inside in terms of energy consumption, although insulation from the inside requires lower investment costs and therefore provides a shorter payback time. With both alternatives, the water vapour condensation potential is negligible. A further interesting outcome is that the use of thermal insulation may result in higher cooling energy requirements, particularly in moderate Oceanic climates [24]. In such situations, increased cooling needs may not compensate decreased heating [25]. This is known as anti-insulation behaviour in the literature, and has also been highlighted by other authors. Masoso and Grobler [26] applied the dynamic software EnergyPlus to a case study in Botswana to demonstrate that anti-insulation behaviour may occur if the cooling set-point temperature is increased. Moreover, Idris and Mae [27] reported that a correlation exists between the wall configuration and the occurrence of anti-insulation behaviour; however, this correlation is also strongly dependent on the external climate and building occupancy profiles [27].

Apart from the latter considerations, given a constructive technique, one may determine the layer sequence that allows for the optimum dynamic thermal behaviour [28,29]. The optimum dynamic thermal behaviour is usually obtained with minimisation of the decrement factor and maximisation of the time lag. Although these two aims cannot be met simultaneously, it has been shown that a symmetric three-layer wall, consisting of a high capacity layer between two equal insulating layers, provides a highly effective solution to satisfy both requirements [30].

In this paper, the authors intend to contribute to the understanding of how to control the dynamic thermal performances of different light and heavy plastered concrete external walls that are in common use. Differently from previously cited studies, where usually a discrete set of alternatives is considered, in this work, the effects of continuous variations in the positioning and thickness distribution of the insulation material on the dynamic thermal performance of external walls are investigated, using calculation models based on the heat transfer matrix method applied to practical examples. This allows determining limit values for thickness and location of insulation layers so that a threshold dynamic thermal transmittance is not exceeded. It is just the continuous variation of the optimization parameters that allows appreciating the subtle interplay between thickness and positions of insulation layers and surface mass of capacitive layers. It is shown that even for light walls, the dynamic thermal transmittance can be kept below prescribed threshold values, if proper thickness and location of insulation layers are employed.

Usually the effect of internal walls is not accounted for when dealing with performance parameters as decrement factor and time lag. However, especially when playing around limit values of the performance parameters, this additional effect deserves to be addressed. In this work, the heat transfer matrix approach is extended to include internal walls and to quantify how they affect the overall room behaviour. An original correlation is proposed, which allows for correction of the dynamic thermal transmittance and time lag of external walls, to take into consideration the effects of the internal walls (partition walls and slabs) on the dynamic thermal behaviour of a room. The results provided in the paper can be used as a guideline for the improvement of dynamic thermal performance of multi-layered walls during the building envelope design stage. The possibility also exists of employing the results provided to devise the most appropriate retrofit actions to be applied to existing buildings, where constraints imposed by costs or preservation aims must be considered.

2- Dynamic thermal performance of multi-layered external walls by heat transfer matrix method

The heat transfer matrix method, also referenced as thermal quadrupole method, is widely used and applied for describing heat conduction in one-dimensional structures [31,32]. As such, it has been widely tested and validated by comparison with experiments [33], or against recognized software tools such as TRNSYS [34]. A preliminary validation of the correct implementation of the heat

transfer matrix method has been performed by comparing its predictions with the results of a control-volume based numerical integration of the one-dimensional heat conduction equation, in a Crank-Nicolson scheme. In this Section and in the following one, this method is used to derive the wall performance parameters that will be applied in Sections 4 and 5.
Consider an external building wall (see Figure 1). The external temperature is assumed to oscillate in time with an amplitude of T_e around the average value of T_{e0}, with the oscillations being characterised by an angular frequency of ω and a period of $P=2\pi/\omega$. In the following, complex formalism will be applied to illustrate oscillating quantities, and the factor $e^{j\omega t}$ will be taken as implicit ($j=\sqrt{-1}$).

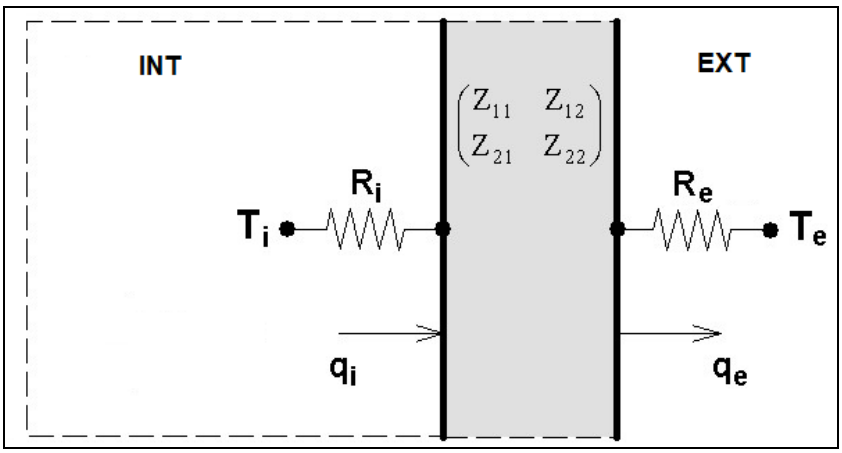

Figure 1- Schematisation of external wall.

The internal room temperature will also generate oscillations, exhibiting the same angular frequency and a complex amplitude of T_i around the average value of T_{i0}. The internal wall side complex amplitudes T_i (relating to the temperature) and q_i (relating to the heat flux) are linearly related to the corresponding external wall side physical quantities T_e and q_e, as follows:

$$\begin{pmatrix} T_i \\ q_i \end{pmatrix} = \begin{pmatrix} Z_{11} & Z_{12} \\ Z_{21} & Z_{22} \end{pmatrix} \begin{pmatrix} T_e \\ q_e \end{pmatrix} = Z \begin{pmatrix} T_e \\ q_e \end{pmatrix} \tag{1}$$

where Z represents the wall transfer matrix.
In the case of a multi-layered wall consisting of a sequence of N homogeneous layers, the transfer matrix can be evaluated as follows:

$$Z = Z_i \left(\prod_{n=1}^{N} Z_n \right) Z_e \tag{2}$$

where Z_n is the transfer matrix of the generic n-th layer (see Figure 2), and Z_i and Z_e are defined as indicated in Figure 2.
If d_n, ρ_n, λ_n and c_n are the values of thickness (m), density (kg/m^3), thermal conductivity (W/mK) and specific heat, respectively, at a constant pressure (J/kgK) related to the n-th homogeneous layer (with thermal resistance $R_n=d_n/\lambda_n$ and surface thermal capacity $C_n=\rho_n d_n c_n$), the corresponding Z_n matrix elements will be given by the International Standard [31], as follows:

$$Z_{n,11} = Z_{n,22} = \cosh(\mathrm{A}_n) \quad ; \quad Z_{n,12} = Z_{n,21} \cdot R_n^2 / \mathrm{A}_n^2 = (R_n / \mathrm{A}_n) \cdot \sinh(\mathrm{A}_n) \tag{3}$$

with $\mathrm{A_n}=(j\omega R_n C_n)^{1/2}$.

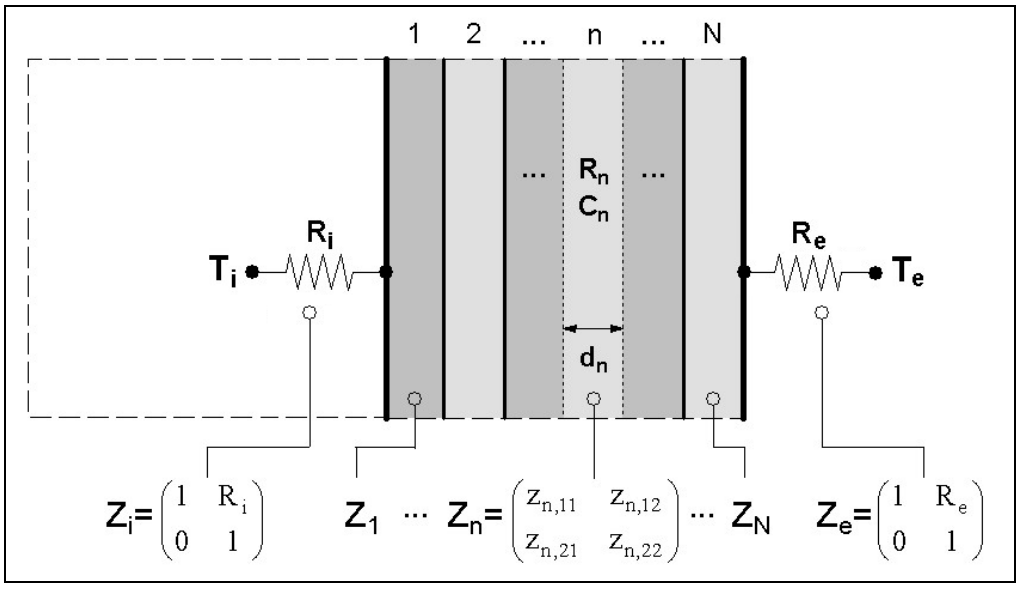

Figure 2- Schematisation of multi-layered wall.

Generally, in the sequential product of Eq. (2), purely resistive layers coincide with the first and last, defined by resistances R_i and R_e, which indicate the internal and external surface thermal resistances, respectively (see Figure 2). The total thermal resistance of the wall, R (m^2K/W), measured between the internal and external air, and the total thermal capacity, C (J/m^2K), will then be given by:

$$R = R_i + \sum_{n=1}^{N} R_n + R_e \quad ; \qquad C = \sum_{n=1}^{N} C_n \tag{4}$$

Other than in the case of matrices representing purely resistive or capacitive layers, the product of the matrices in Eq. (2) are normally not commutative, making the layer sequence order essential.
Generally, matrices characterising different homogeneous layers are commutable only if the ratio between the thermal capacity and thermal resistance is the same for each layer; that is, if C_n/R_n, or the thermal effusivity $E_n = \sqrt{\lambda_n \rho_n c_n}$ is constant for all layers [32,36].
Under the hypothesis of the isothermal boundary condition (T_i=0), the dynamic thermal transmittance Y_{ie}, decrement factor f_a and time lag φ can be defined as follows [14,22,30]:

$$Y_{ie} = 1/|Z_{12}| \quad ; \qquad f_a = Y_{ie} \cdot R \quad ; \qquad \varphi = P/2\pi \cdot \arg(1/Z_{12}) \tag{5}$$

The dynamic thermal insulation provided by the external wall will be greater (that is, the reliance of internal room conditions on external conditions will be smaller) with a smaller dynamic thermal transmittance Y_{ie} (and therefore decrement factor f_a) and a greater time lag φ [22,37,38]. It is therefore of considerable importance to search for the optimal layer sequence of a given wall, with the aim of minimising Y_{ie} and maximizing φ (see also Appendix A). It should be noted that Z_{12} remains invariant under a specular reflection of the entire wall; that is, a reflection obtained by a completely reversed layer ordering. Such a symmetry property has significant consequences. If, as seems reasonable, according to variations in the layer sequence and therefore in the resistance-capacity distribution, there exists only one wall that is optimal for Y_{ie} (for which $|Z_{12}|$ reaches its maximum value and Y_{ie} therefore its minimum), this wall must necessarily be symmetric by reflection. In fact, if such an optimal wall were not symmetric, it would be possible to obtain two walls with the same Y_{ie} value by specular reflection; such walls would be distinct, and both optimal for Y_{ie}. If it exists and is unique, the optimal wall for Y_{ie} is necessarily symmetric by reflection.

Similar considerations can also be made for the layer sequence maximising the time lag φ, which is only dependent on the matrix element Z_{12}. All of this leads us to exclude, as optimal, walls that are realised with two layers (apart from possible plaster layers), which are obviously non-symmetric and obtained by installing all the insulating material either on the external side (insulation from the outside) or internal side (insulation from the inside).
In this study, the problem of determining the optimal layer sequence for a given multi-layered wall is solved, demonstrating that it is normally not possible to optimise the layer sequence in such a way as to minimise Y_{ie} and simultaneously maximise φ.

3- Influence of internal walls by heat transfer matrix method

The thermal comfort of a building depends not only on the envelope structures (facades and roofs), but also the internal structures (partition walls and slabs). This becomes particularly evident if the passive behaviour of the building is studied, that is, the manner in which the building reacts to external temperature variations when no air conditioning system is operating. The question involved is of great relevance. In fact, it should be noted that a building that has been the object of an effective thermal design, so as to exhibit excellent passive behaviour, can provide a satisfactory comfort level in the summer, even when no air conditioning system is installed or, at most, when the role of that system is limited, with significant energy consumption savings.

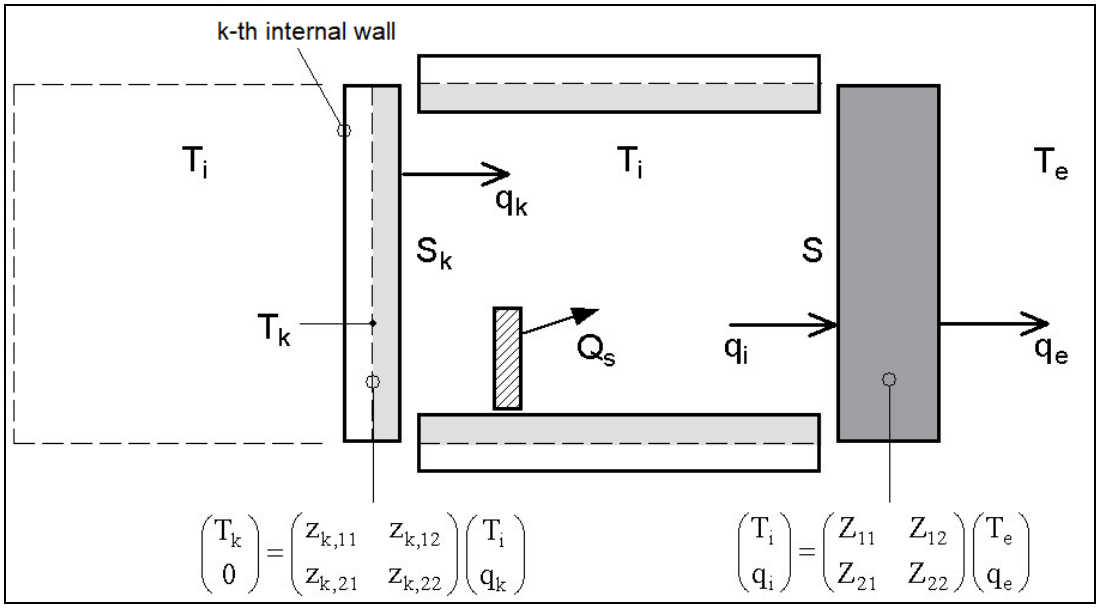

Figure 3- Schematisation of analysed room.

Figure 3 illustrates the outline of a room with both external and internal (partition walls and slabs) walls that are multi-layered. The external room wall has a surface S; the internal portion of the room consists of K internal structures (partition walls and slabs), of which the generic section has a surface S_k. The room includes a thermal source (provided, for example, by an air conditioning system). Let Q_S be the thermal power per surface unit of the external wall, provided by the thermal source, and the sol-air temperature $T_e(t)$ be the reference external temperature [39]. As the assumed thermal transmission is one-dimensional, any effects resulting from thermal bridges will be neglected. Under dynamic thermal conditions, characterised by a period P, the external wall remains within the applicability of [35], from which the following equation can be derived:

$$q_i = Y_{12}\, T_e + Y_{22}\, T_i \qquad (6)$$

with $Y_{12}=-1/Z_{12}$ and $Y_{22}=Z_{22}/Z_{12}$.
In many cases, the generic internal wall can be outlined as symmetric; its function is to divide rooms sharing the same thermal regime (see Figure 3). Under such conditions, the surface passing through the *k-th* wall's midspan at a temperature T_k can be outlined as adiabatic. Consequently, the only portion affected by the thermal balance within the room is the half of the wall giving onto the room itself.
As far as the *k-th* internal wall is concerned, the linear relationship will appear as follows:

$$\begin{pmatrix} T_k \\ 0 \end{pmatrix} = \begin{pmatrix} z_{k,11} & z_{k,12} \\ z_{k,21} & z_{k,22} \end{pmatrix} \begin{pmatrix} T_i \\ q_k \end{pmatrix} \tag{7}$$

from which, in particular:

$$q_k = -(z_{k,21} / z_{k,22}) T_i = -\ell_k T_i \tag{8}$$

illustrating the added admittance ℓ_k as a property of the *k-th* internal wall, defined by:

$$\ell_k = z_{k,21} / z_{k,22} \tag{9}$$

By neglecting the effects due to air change, air inside the room and furnishing elements, the simple balance equation relating to the external wall surface unit can be expressed by:

$$q_i = Q_i + Q_S \tag{10}$$

where Q_i represents the total heat flux affecting the internal structures, and can be calculated as follows:

$$Q_i = \frac{1}{S} \sum_{k=1}^{K} S_k \, q_k = -T_i \sum_{k=1}^{K} \ell_k \, v_k = -T_i \, \Lambda \tag{11}$$

where $v_k=S_k/S$ indicates the 'weight' of the *k-th* internal wall and Λ, known as the total admittance relating to the internal structures (dependent on the room structure and geometry), is defined by:

$$\Lambda = \sum_{k=1}^{K} \ell_k \, v_k \tag{12}$$

When no air conditioning system is operating and the intention is to study the purely passive indoor behaviour, from Eq. (10) with $Q_S=0$ and using Eqs. (6) and (11), the ratio ζ obtained between the internal and external temperature is given by:

$$\zeta = (T_i / T_e) = 1/(Z_{22} + Z_{12} \, \Lambda) \tag{13}$$

Compared to external temperature variations, internal temperature variations will be diminished by a decrement factor μ and time lag ψ, represented by:

$$\mu = |\zeta| \quad ; \quad \psi = (P / 2\pi) \arg(Z_{22} + Z_{12} \, \Lambda) \tag{14}$$

with $0 \leq \arg(Z_{22}+Z_{12} \, \Lambda) \leq 2\pi$. The parameters μ and ψ can be regarded as performance indices for the room under examination. It should be noted that the first part of Eq. (14) can be expressed in the following form:

$$\mu = Y_{ie} / |Y_{22} + \Lambda| \tag{15}$$

It is obvious that μ and ψ depend on the external wall thermal properties through the matrix elements Z_{12} and Z_{22}, the internal structure thermal properties through Λ and the period P relating to the external temperature variations. The dynamic thermal insulation effect will be greater (that is, the reliance of the internal room conditions on the external conditions will be smaller) with a smaller μ and greater time lag ψ.
Finally, it should be noted that, by assuming $T_i=0$ from Eqs. (10) and (11), the following can be obtained:

$$Q_i=0 \quad ; \quad |Q_S| = Y_{ie}\, T_e \tag{16}$$

From Eq.(16) it is clear that smaller Y_{ie} results in lower thermal power to be provided by the air conditioning system, to maintain a constant room temperature. However, it is important to note that in the present study the analysis is focused on the dynamic passive behaviour of the building. This is an important aspect, especially moving towards modern and very energy efficient buildings, in which the role of the air conditioning system is required as marginal as possible [40]. The analysis aimed at optimizing the layer sequence with a working air-conditioning system was studied in previous works by some of the same authors and requires the introduction of different parameters, also including performance parameters of the air-conditioning system, such as the response length and the temporal behaviour [30,41,42].
Certain relevant problems relating to the building dynamic thermal behaviour can be expressed as follows. For a room with a given internal structure admittance Λ, the problem is how to determine: the external wall stratigraphy, with assigned values of R and C, aimed at minimising the decrement factor μ, and the external wall stratigraphy, with assigned values of R and C, aimed at maximising the time lag ψ. In this case it should be noted that, as a rule, as opposed to what has been discussed about external structures, for Eq. (15), the internal wall optimal layer sequence depends not only on the dynamic thermal transmittance, but also on both the external wall admittance and Λ. Given the significant relevance of the performance indices μ and ψ (considering the influence of internal walls) to determine the building thermal passive behaviour, the legislation on building energy performance for each European country should set limit values for these indices.

4- Examples of dynamic thermal performance of light and heavy plastered concrete external walls

The analytical method proposed in Section 2 was used to analyse the manner in which the resistive layer placements and capacitive layer properties affect the summer thermal performance of the wall. The calculations were made in *MAPLE* software, assuming a daily period (P=24 h) for the external temperature variations. It should be remembered that, in the Italian national legislation decrees [43], in the case of towns where the monthly average value of solar radiation intensity exceeds 290 W/m^2, opaque vertical walls (facing south, south-west, west, south-east and east) must comply with at least one of the following requirements: the surface mass value M_s (evaluated excluding plaster layers) must be higher than $M_{s,lim}$=230 kg/m^2 or the dynamic thermal transmittance value Y_{ie} must be lower than $(Y_{ie})_{lim}$=0.10 W/m^{2}K.

4.1- Impact of layer sequence

The first example is focused on studying the impact of how the layer sequence on the dynamic thermal performance of three light external walls (*P1*, *P2* and *P3*), with $M_s<M_{s,lim}$, and one heavy wall (*PT*), with $M_s>M_{s,lim}$. The thermo-physical properties of the materials used (density ρ, thermal conductivity λ, specific heat c and thermal diffusivity α) are displayed in Table 1. As a reference, all the data in Table 1 were obtained from the European Standards [44,45]. In Table 2, the following are indicated for each wall: concrete type and thickness d_C, thermal insulation thickness d, total thickness D, surface mass M_s, surface thermal capacity C and thermal transmittance U. Regarding

the internal and external surface thermal resistances in summer heat transfer conditions, the following reference values were considered [35]: R_i=0.13 m^{2}K/W and R_e=0.07 m^{2}K/W. All the walls were constructed by combining the concrete structure (types A, B, C and D) with an insulating layer and two layers of 1-cm-thick plaster (top coat plaster layers).

Despite sharing the same thermal transmittance value U≅0.32 W/m^{2}K, and obviously the same thermal resistance value $R=1/U$≅3.13 m^{2}K/W, the walls exhibit different surface mass values, as follows: *PT* wall with $M_s>M_{s,lim}$; *P1* wall with M_s≅2/3 $M_{s,lim}$; *P2* wall with M_s≅1/2 $M_{s,lim}$; and *P3* wall with M_s≅1/3 $M_{s,lim}$. For each wall, four-layer sequences, represented schematically in Figure 4, were considered: *SC*, insulation from the outside; *SI*, insulation from the inside; *SS*, insulation in the cavity; and *SE*, insulation on both sides. For useful comparisons, an additional sequence order *SO* (see Fig. 4) was considered, and obtained with an equivalent homogeneous layer, constructed with uniformly distributed thermal capacity and conductive thermal resistance. The combination of four walls and five sequence layer orders allowed for the analysis of 20 different building structures.

Material		**ρ** (kg/m^3)	**λ** (W/mK)	**c** (J/kgK)	**α** (m^2/Ms)
Traditional plaster (lime and sand mortar)		1600	0.80	1000	0.50
Concrete blocks	**A** type (expanded clay)	1200	0.43	880	0.41
	B type (expanded clay)	1000	0.33		0.38
	C type (autoclaved cellular)	800	0.28		0.40
	D type (autoclaved cellular)	500	0.20		0.45
Thermal insulation (e.g. glass wool)		70	0.034	1030	0.47

Table 1- External walls: thermo-physical properties of different layers.

Wall	**Concrete**		**Thermal insulation**	**Main properties**			
	Type	**d_C** (cm)	**d** (cm)	**D** (cm)	**M_s** (kg/m^2)	**C** (kJ/m^{2}K)	**U** (W/m^{2}K)
PT	**A**	24	8	34	294	291	0.319
P1	**B**	18	8	28	186	196	0.320
P2	**C**	16	8	26	134	150	0.318
P3	**D**	16	7	25	85	107	0.324

Table 2- Main properties of analysed walls: *PT* heavy wall (M_s>230 kg/m^2), and *P1*, *P2* and *P3* light walls (M_s<230 kg/m^2). Each configuration is composed of a layer of concrete (variable thickness) and a layer of thermal insulation (7-8 cm thick).

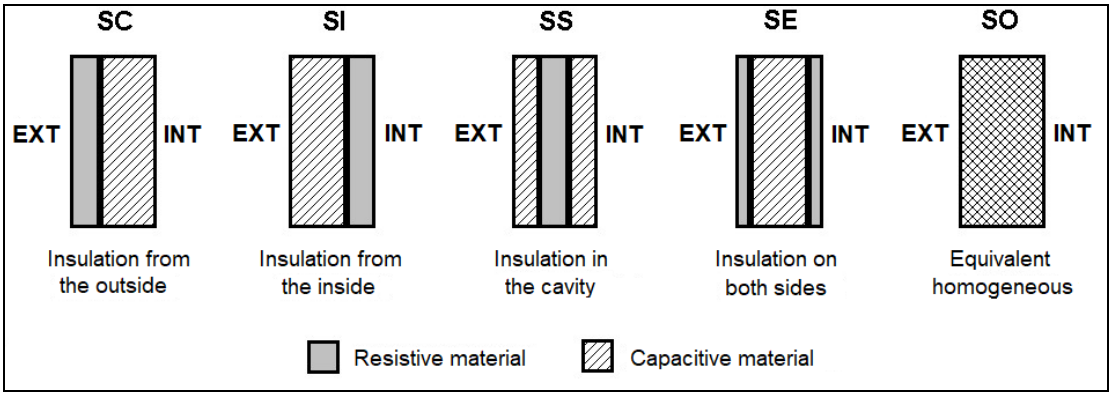

Figure 4- Schematic representation of layer sequences of analysed walls (top coat plaster layers are not represented).

In Figure 5, the results of the evaluation of performance parameters φ and Y_{ie}, related to the four analysed walls *PT*, *P1*, *P2* and *P3*, are shown for all five-layer sequences *SC*, *SI*, *SS*, *SE* and *SO* (see also the example discussed in Appendix A). The values of the performance parameter f_a are directly proportional to Y_{ie} and they can be easily evaluated using Eq. (5), considering the value of *R* (3.13 m^2K/W) equal for all the analysed walls. In the top part of Figure 5, the values φ=8 h and φ=12 h are highlighted: according to the Italian legislation they represent the minimum values for a wall to achieve good and excellent dynamic thermal performance respectively. In the bottom part of Figure 5, the value of $(Y_{ie})_{lim}$=0.10 W/m^2K is highlighted. In Figure 5 it can be observed that optimal dynamic performances are obtained for all walls in the case of the *SE* layer sequence (provided with materials which, being characterised by essentially capacitive thermal properties, are centrally placed between two thermal insulation layers), whereas the worst dynamic performances are obtained in the case of the *SS* layer sequence. In current construction practices, walls characterised by the *SE* layer sequence are being built according to different construction technologies; for example, based on using thermal insulating disposable formworks, where wet concrete is poured in situ, embedded insulation concrete or clay blocks.

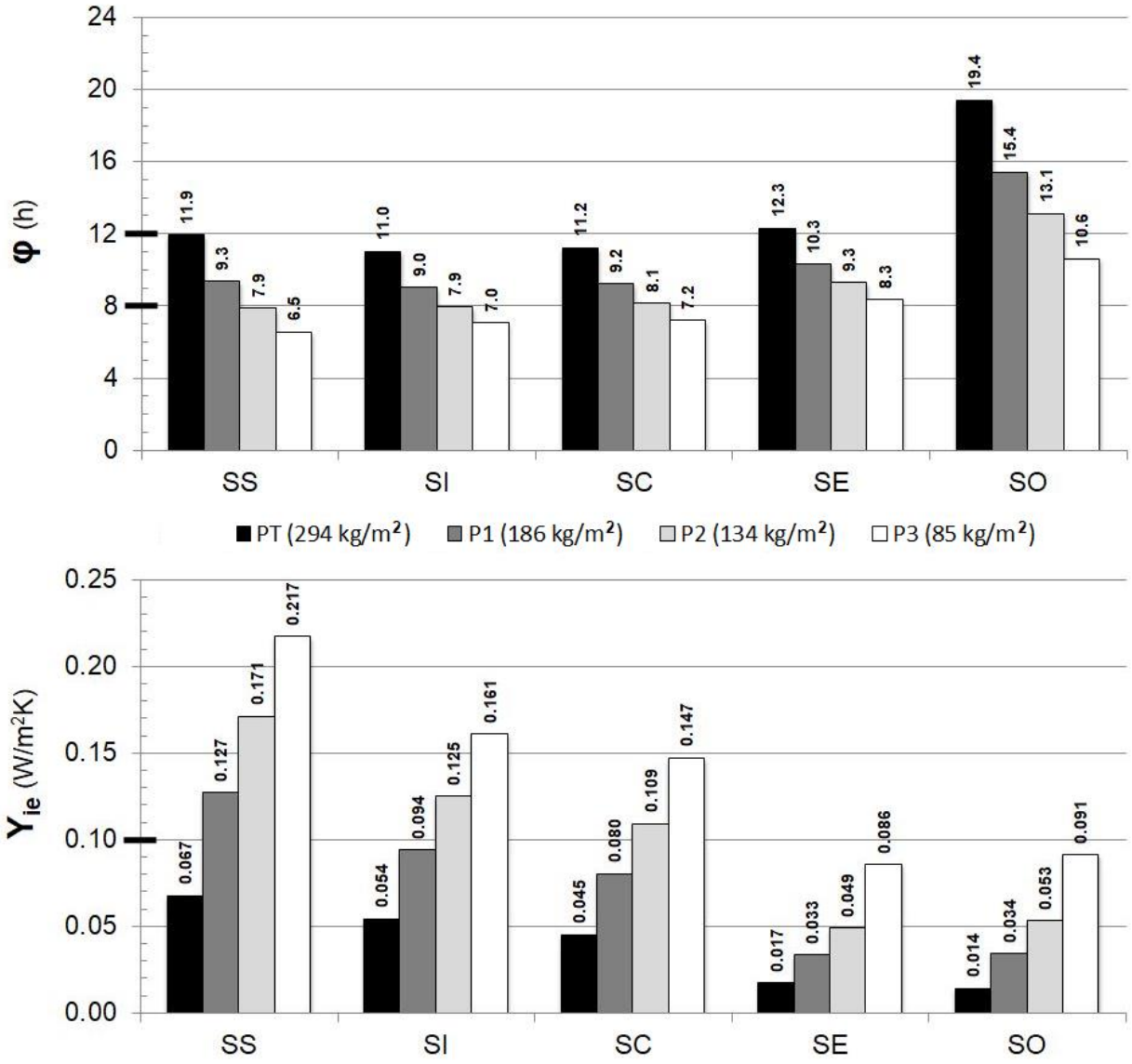

Figure 5- Calculated values of time lag φ (top) and dynamic thermal transmittance Y_{ie} (bottom). The results obtained for the analysed walls (*PT, P1, P2, P3*) are displayed for all the different layer sequences (*SS, SI, SC, SE* and *SO*).

For each layer sequence, the heavy wall *PT* (with $M_s > M_{s,lim}$) complies with the Italian legislative requirement $Y_{ie} < (Y_{ie})_{lim}$ and reaches values of φ higher than 8 h. The light walls *P1*, *P2* and *P3* (for all of which $M_s < M_{s,lim}$) comply with such a limit depending on where and how the insulating layer is placed: as the wall surface mass decreases, the insulating layer becomes more relevant in terms of placement and thickness. However, the aim of improving the light wall summer performance parameters (Y_{ie}, but also f_a and φ) is attained by devoting special design efforts to selecting a suitable insulation type, considering its thickness and placement inside the wall. For example, having to make constructive choices, it is preferable to have a *P2* wall (light solution, $M_s < M_{s,lim}$) with *SE* layer sequence, rather than a *P1* (heavy solution, $M_s > M_{s,lim}$) with *SS* and *SI* layer sequences. In Figure 5, it can be also observed that the equivalent homogeneous layer *SO* exhibits excellent behaviour for all the analysed walls compared to the remaining layer sequences *SC*, *SI*, *SS* and *SE*, especially in terms of φ. Therefore, it is particularly advantageous to construct blocks with a distributed thermal insulation [46,47], suitable for approximating the equivalent homogeneous layer *SO*, for both their dynamic thermal performance and ease of installation, which can contribute to simplifying and accelerating in situ works. Particularly regarding the insulating layer thickness, it appears appropriate to draw attention to the following. When attempting to improve performance parameters f_a, φ and Y_{ie}, relating to walls *P2* and *P3*, it appears reasonable to increase the insulating layer thickness. In doing so, due to the negligible increase undergone by their surface mass, the walls will obviously always remain light. However, in this regard it must be noted that, concerning walls *P2* and *P3* even in the case of the best layer sequence *SE*, to obtain f_a and φ values (proportional parameters) fitted for providing excellent dynamic thermal performance, the required thermal insulation thicknesses are very high. In particular, difficulties arise from an attempt to let φ increase significantly in value. For example, to obtain $\varphi > 12$ h (excellent dynamic thermal performance), the required thermal insulation thicknesses exceed 22 cm in the case of *P2* and 25 cm in the case of *P3*, respectively.

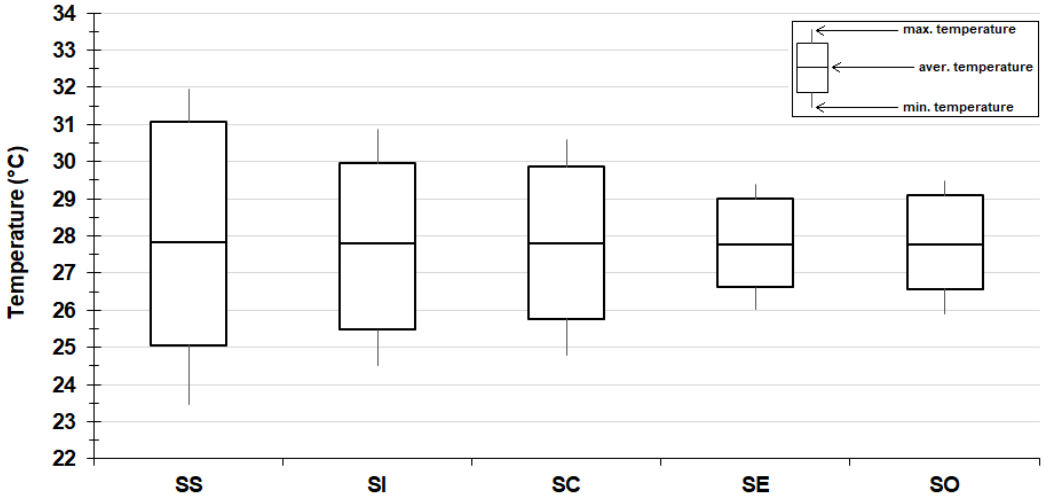

Figure 6- Maximum, minimum and average internal air temperatures for the different analysed rooms. Note that: the external temperature is assumed to oscillate in time with a period of 24 h and an amplitude of 6.3°C around the average value of 27.6°C; for each room the white rectangle represents the temperature range within which the internal temperature remains for 50% of the time.

The heat transfer matrix method, in particular the use of the parameters f_a (or Y_{ie}) and φ, is able to provide general indications also for an evaluation of the internal comfort during the passive behaviour of the building. Considering by way of example the daily trend of the maximum summer external temperature for the city of Rome (representative of the climatic conditions of central Italy

and other Mediterranean areas with similar latitude), evaluated according to the procedure described in the national standard on climatic data (i.e. Italian standardized technical report UNI/TR 10349), it can be approximated by a sinusoidal oscillation in time with a period of 24 h and an amplitude of 6.3°C around the average value of 27.6°C. Using the proposed methodology, daily trends of the internal air temperature were obtained for the 20 different analysed building structures. In Figure 6, maximum, minimum and average values of the internal air temperature are shown for the lightest wall (*P3*), together with the range within which the temperature remains for 50% of the time. For example, from Figure 6 it is possible to notice how the *SE* layer sequence is associated with the smallest oscillation of the internal temperature. The maximum value of the internal temperature of 29.4°C is reached (lower than all the other layer sequences) and that for 50% of the time the internal temperature remains between 26.6 and 29.0°C. The internal air temperature is one of the main parameters that influence the comfort perceived by people within the indoor spaces. Although the heat transfer matrix model described in Section 2 provides only general indications about the internal temperatures, it is very useful for comparing the performance of walls characterized by different surface mass values and different layer sequences, during the early stage of the design process.

4.2-Impact of thermal insulation thickness distribution

The second example focuses on the study of the impact of thermal insulation thickness distribution on the dynamic thermal performance of the analysed multi-layered walls (*PT, P1, P2* and *P3*; see Tab. 2). For this purpose, let η ($0 \le \eta \le 1$) be the fraction of the thermal insulation placed on the internal side of the concrete. Regarding Figure 7: for η =0, all the thermal insulation is placed on the external side of the concrete (*SC* layer sequence; see Fig. 4); for η =1/2, the thermal insulation is equally placed on both the external and internal sides of the concrete (*SE* layer sequence; see Fig. 4); for η =1, all the thermal insulation is placed on the internal side of the concrete (*SI* layer sequence; see Fig. 4). Under such conditions, $\eta \cdot d$ represents the insulation thickness from the inside and $(1-\eta)\cdot d$ the insulation thickness from the outside. Despite the availability of standard thickness insulation materials in the market, continuously varying η are considered to determine limit values that can be assumed by this parameter to obtain Y_{ie} below a prescribed threshold.

Figure 7 illustrates the trend of Y_{ie} as a function of η for all the analysed walls; the horizontal line corresponding to $Y_{ie}=(Y_{ie})_{lim}$ is also highlighted. From Figure 7, it is evident that the dynamic thermal transmittances of the *PT* and *P1* walls remain lower than $(Y_{ie})_{lim}$, regardless of the value of η. The dynamic thermal transmittances are higher than $(Y_{ie})_{lim}$ for $\eta<0.02$ and $\eta>0.94$ in the case of the *P2* wall, and for $\eta<0.22$ and $\eta>0.75$ in the case of the *P3* wall. Each trend exhibits a minimum Y_{ie} value for η very close to 0.5, corresponding to the *SE* layer sequence.

4.3- Impact of thermal insulation placement

The third example focuses on studying the impact of thermal insulation placement on the dynamic thermal performance of the analysed multi-layered walls (*PT, P1, P2* and *P3*; see Tab. 2). For this purpose, let ξ ($0 \le \xi \le 1$) be the fraction of the concrete externally disposed with respect to the thermal insulation. Regarding Figure 8: for ξ =0, the thermal insulation is placed so that all of the concrete is internally disposed (*SC* layer sequence; see Fig. 4); for ξ =1/2, the thermal insulation is placed in the middle of the concrete (*SS* layer sequence; see Fig. 4); for ξ =1, the thermal insulation is placed so that all of the concrete is externally disposed (*SI* layer sequence; see Fig. 4). Under such conditions, $\xi \cdot d_C$ represents the concrete layer thickness from the outside, while $(1-\xi)\cdot d_C$ represents that from the inside. Despite the availability of standard concrete elements in the market, continuously varying ξ values are considered.

Figure 8 illustrates the trend of Y_{ie} as a function of ξ for all analysed walls; the horizontal line corresponding to $Y_{ie}=(Y_{ie})_{lim}$ is also highlighted. From Figure 8, it is evident that the dynamic

thermal transmittances of the *PT* wall remain lower than $(Y_{ie})_{lim}$, and those of the *P2* and *P3* walls remain higher than $(Y_{ie})_{lim}$, regardless of the value of ξ. Moreover, the dynamic thermal transmittances of the *P1* wall are higher than $(Y_{ie})_{lim}$ for ξ<0.15 and ξ>0.95. All walls reach their maximum Y_{ie} for a ξ value close to 0.5, corresponding to the *SS* layer sequence.

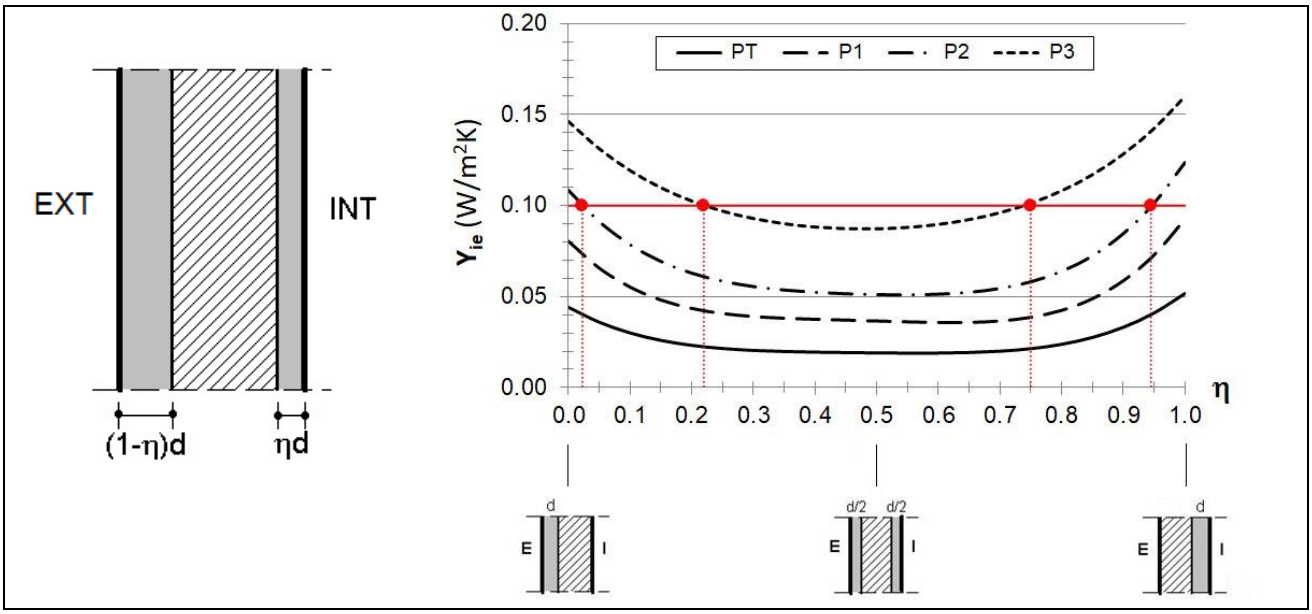

Figure 7 – (Left) Schematic representation of thermal insulation thickness distribution (dark coloured material is the thermal insulation, material with diagonal lines is the concrete, plaster layers are not represented). (Right) Trend of Y_{ie} as function of η for all analysed walls.

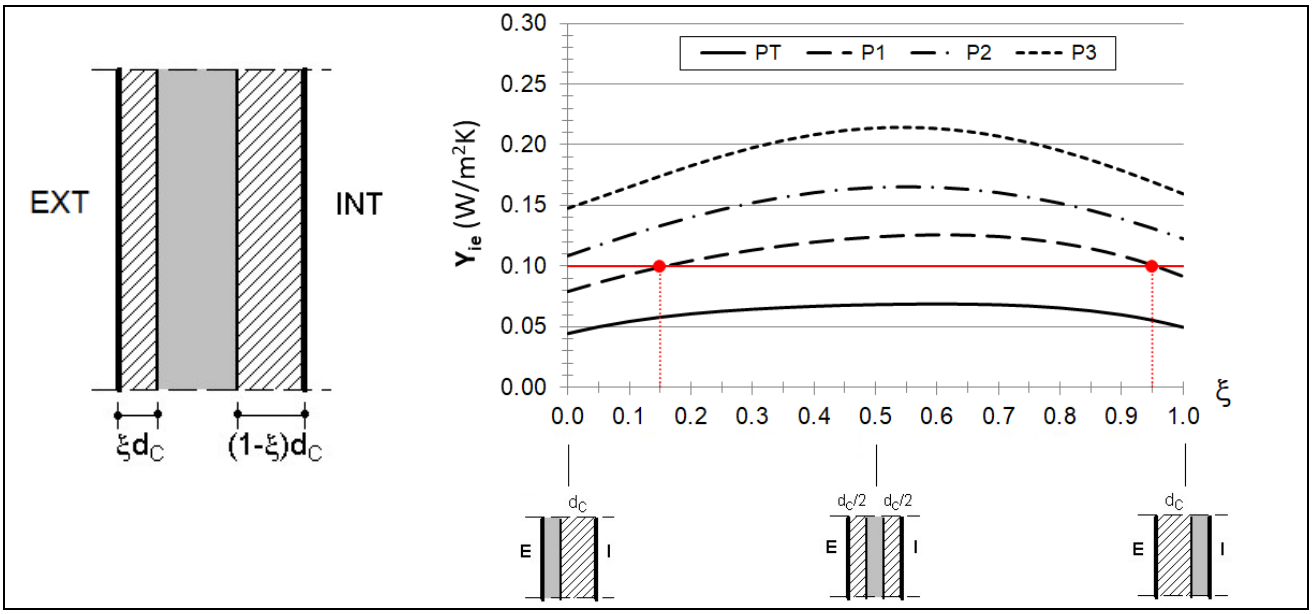

Figure 8 – (Left) Schematic representation of thermal insulation placement (dark coloured material is the thermal insulation, material with diagonal lines is the concrete, plaster layers are not represented). (Right) Trend of Y_{ie} as function of ξ for all analysed walls.

5- Examples of influence of internal walls on room passive thermal behaviour

The analytical method proposed in Section 3 was used to analyse the influence of internal walls on the passive behaviour of a room. The calculations were made in *MAPLE* software, assuming a daily period (*P*=24 h) for the external temperature variations. To develop the analysis, a room with a single external wall (schematised in Figure 9) was consider, it is defined by the following

dimensions: 4 m length, 4 m width and 2.70 m height,. According to the symbols in Figure 9, the following values can be calculated: S=10.8 m^2 and V=43.2 m^3. The average value R_i=0.13 m^{2}K/W is used for the internal thermal surface resistance. Traditional heavy internal walls are considered for the analysis, as indicated in Table 3. In the table, the materials considered for the different layers are indicated with their respective thicknesses (d) and thermo-physical properties (ρ, λ, c, α). Considering the data in Table 3, for P=24 h, the total admittance of the internal walls is equal to $\Lambda=23.78+15.88\,j$, which implies: $|\Lambda|$=28.60 W/m^{2}K.

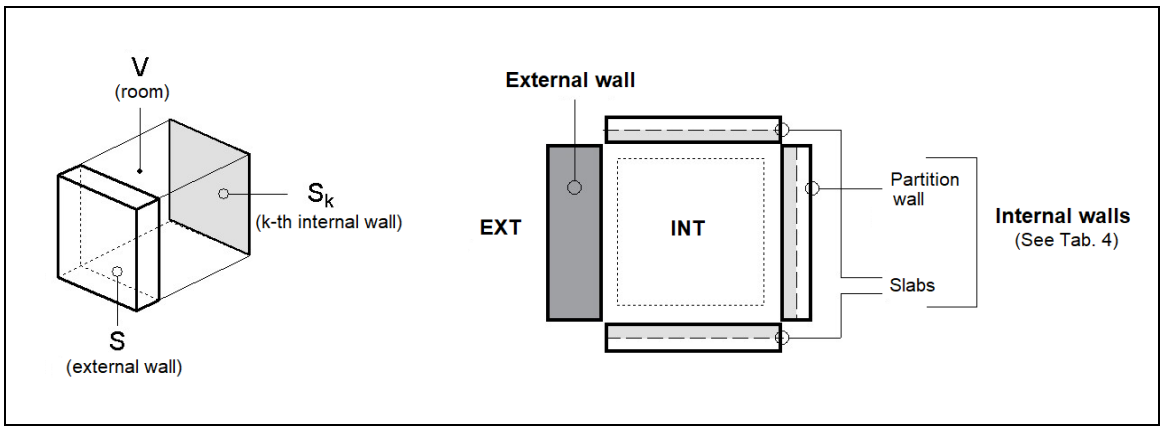

Figure 9- (Left) Schematisation of room. (Right) Exemplification of case study.

Internal wall	Material	d (cm)	ρ (kg/m^3)	λ (W/mK)	c (J/kgK)	α (m^2/Ms)
Partition walls	Plaster	1.0	1600	0.80	1000	0.50
	Brick	12	1200	0.43	850	0.42
	Plaster	1.0	1600	0.80	1000	0.50
Slabs	Concrete	20	2200	1.16	900	0.59

Table 3- Internal walls: thermo-physical properties of the different layers.

External wall	Layer sequence	Room		
(See Tab.2 and Fig. 4)		ID	μ·10^2	ψ (h)
PT	SC	1	0.139	13.4
	SI	2	0.182	13.3
	SE	3	0.0578	14.6
P1	SC	4	0.250	11.4
	SI	5	0.316	11.3
	SE	6	0.111	12.6
P2	SC	7	0.341	10.4
	SI	8	0.421	10.2
	SE	9	0.163	11.6
P3	SC	10	0.468	9.50
	SI	11	0.539	9.36
	SE	12	0.286	10.6

Table 4- Dynamic thermal properties of considered rooms.

In Table 4, the calculated values of the parameters μ and ψ are displayed for 12 different rooms. The different rooms are obtained by using the internal walls (partition walls and slabs) indicated in Table 3 and combining the wall types *PT*, *P1*, *P2* and *P3* with the layer sequences *SC*, *SI* and *SE* to create different external walls.
If the values of parameters Y_{ie} and φ (relating to the external walls; see Figure 5) are compared to the values of μ and ψ (relating to the room; see Tab. 4), it is evident that μ decreases with a decreasing Y_{ie}, while ψ increases with an increasing φ for all analysed external walls. These results confirm that the comments made previously regarding optimisation of the layer sequence of an external wall are also valid for optimisation of the parameters μ and ψ for a room provided with given internal structures, in particular the rooms that have an external wall realized with *SE* layer sequence (*ID* 3,6,9, and 12) are characterized by μ values lower than 40% and ψ values higher of about 10% if compared to the average values of the respective parameters calculated with the other sequences.
In terms of both the room under examination and numerous practically interesting cases, the total admittance modulus relating to the internal walls $|\Lambda|$ is sufficiently wide ($R|\Lambda|>>1$) to allow the following approximation for Eqs. (14) and (15):

$$\mu \cong 1/|Z_{12}\Lambda| = Y_{ie}/|\Lambda| \quad ; \quad \psi \cong (P/2\pi)\arg(Z_{12}\Lambda) = \varphi + t \tag{17}$$

with $t=(P/2\pi)\arg(\Lambda)$, which in the case of the analysed room is t=2.2 h.
By using the previous relations and the $|\Lambda|$ and t values obtained for the analysed room, we can easily verify that it is possible to derive the μ and ψ values indicated in Table 4 from the Y_{ie} and φ values indicated in Figure 5 with excellent accuracy.

6- Conclusions

The external walls of buildings are generally multi-layered and, as highlighted by numerous studies found in the literature, the layer thicknesses, properties and positions have a significant influence on the overall dynamic thermal behaviour of the walls. The dynamic thermal performances of walls are usually characterised by the dynamic thermal transmittance, decrement factor and time lag.
In this study, the thermal performances of external walls were analysed under dynamic conditions, by using the heat transfer matrix method. The analysis was focused on the impact of the layer sequence, thermal insulation thickness distribution and thermal insulation placement on the dynamic performance of light and heavy plastered concrete external walls, from a surface mass of 85 kg/m^2 to a surface mass of 294 kg/m^2. The differences between the dynamic thermal transmittances, decrement factors and time lags of 20 different walls, characterized by the same value of thermal transmittance, were discussed quantitatively. As opposed to general methods in the literature, the impacts of continuous variations in the insulation thickness distribution and insulation thickness placement were analysed, and original trends of the dynamic thermal transmittance were illustrated. These trends can be highly useful (as guide abacuses) during early stages of the design process, when important decisions on constructive strategies and techniques must be made by architects, engineers or other technical figures devoted to energy-efficient design. The main achieved results can be summarized as follows.

- Optimal dynamic performances are obtained, for all analysed walls, with the thermal insulation placed on both sides of the capacitive material (concrete), whereas the worst dynamic performances are obtained with the thermal insulation placed between two layers of capacitive material. Quantitatively, for the lightest analysed wall (85 kg/m^2) the choice of the layer sequence (on both sides or in the cavity) implies the increase of the dynamic thermal transmittance from 0.086 to 0.217 W/m^{2}K; in Italy, this means being compliant or not compliant with the building energy performance legislation (dynamic thermal transmittance lower than 0.1 W/m^{2}K) having used the same materials (concrete and thermal insulation) and in the same

quantities. For each layer sequence, the heaviest analysed wall (294 kg/m^2) complies with the Italian legislative requirement and its time lag values exceed 8 h (threshold value to confer good level to the dynamic performance according to Italian legislation) and in some cases 12 h (threshold value to confer excellent level to the dynamic performance).

- Having to make constructive choices, it is favourable to have a lighter solution (e.g. 134 kg/m^2), with thermal insulation on both sides, rather than to have a heavier solution (e.g. 294 kg/m^2) with thermal insulation in the cavity: these two solutions are characterized by dynamic thermal transmittance values of 0.033 and 0.067 W/m^{2}K respectively (one about the half than the other) and time lag values both in the range from 8 to 12 h (good dynamic performance).
- The impacts of the thermal insulation thickness distribution and of the thermal insulation placement on the dynamic thermal performance of the wall become increasingly important as the weight of the wall is reduced. For the lightest analysed wall, in order not to exceed by more than 15% the minimum obtained value of dynamic thermal transmittance (equal to 0.086 W/m^{2}K with equally distributed thermal insulation between outside and inside) it is possible to choose a solution that requires to place on the internal side from a minimum of 35% to a maximum of 65% of the insulation thickness. In the case of the use of a single thermal insulation layer, for the lightest analysed wall, the placement of this layer on the external side, compared to the placement in the cavity, allows a reduction on the value of dynamic thermal transmittance by more than 30%, while the placement on the internal side a reduction of about 25%.

Moreover, the authors proposed a simplified method, based on the correction of the decrement factor and time lag values, to evaluate the influence of internal walls (partition walls and slabs) on indoor thermal comfort, in the case of no air conditioning system operating. The presented results demonstrate that optimization of an external wall layer sequence also applies when considering the influence of the internal partitions. The proposed methodology may be useful for the design stage of new buildings, as well as for the evaluation of retrofitting actions of existing buildings, to have a fast estimation of the passive dynamic behaviour of a room, without the need to carry out detailed simulations of dynamic energy behaviour, which usually take place at a very advanced stage of design.

References

[1] Directive 2010/31/EU of the European Parliament and of the Council of 19 May 2010 on the energy performance of buildings, available at:
http://eur-lex.europa.eu/legal-content/EN/TXT/PDF/?uri=CELEX:32010L0031&from=EN

[2] "Energy Renovation: The Trump Card for the New Start for Europe", European Commission Joint Research Centre's report, available at:
http://publications.jrc.ec.europa.eu/repository/bitstream/JRC92284/eur26888_buildingreport_online_2015-03-25.pdf

[3] G. A. Florides, S. A. Tassou, S. A. Kalogirou, L. C. Wrobel, Measures used to lower building energy consumption and their cost effectiveness, Applied Energy 73 (2002) 299-328.

[4] Y. Huang, J. Niu, T. Chung, Study on performance of energy-efficient retrofitting measures on commercial building external walls in cooling-dominant cities, Applied Energy 103 (2013) 97-108.

[5] A. Reilly, O. Kinnane, The impact of thermal mass on building energy consumption, Applied Energy 198 (2017) 108-121.

[6] P. Dongmei, C. Mingyin, D. Shiming, L. Zhongping, The effects of external wall insulation thickness on annual cooling and heating energy uses under different climates, Applied Energy 97 (2012) 313-318.

[7] K. J. Kontoleon, C. Giarma, Dynamic thermal response of building material layers in aspect of their moisture content, Applied Energy 170 (2016) 76-91.

[8] S. Verbeke, A. Audenaert, Thermal inertia in buildings: A review of impacts across climate and building use, Renewable and Sustainable Energy Reviews 82 (2018) 2300-2318.

[9] R. J. Duffin, A passive wall design to minimize building temperature swings, Solar Energy 33 (1984) 337-342 .

[10] R. J. Duffin, G. Knowles, Use of layered walls to reduce building temperature swings, Solar Energy 33 (1984) 543-549.

[11] P.T. Tsilingiris, Thermal flywheel effects on the time varying conduction heat transfer through structural walls, Energy and Buildings 35 (2003) 1037-1047.

[12] P. T. Tsilingiris, Parametric space distribution effects of wall heat capacity and thermal resistance on the dynamic thermal behavior of walls and structures, Energy and Buildings 38 (2006) 1200-1211.

[13] H. Asan, Effects of wall's insulation thickness and position on time lag and decrement factor, Energy and Buildings 28 (1998) 299-305.

[14] H. Asan, Investigation of wall's optimum insulation position from maximum time lag and minimum decrement factor point of view, Energy and Buildings 32 (2000) 197-203.

[15] E. Kossecka, J. Kosny, Influence of insulation configuration on heating and cooling loads in a continuously used building, Energy and Buildings 34 (2002) 321-331.

[16] S. A. Al-Sanea, M. F. Zedan, Improving thermal performance of building walls by optimizing insulation layer distribution and thickness for same thermal mass, Applied Energy 88 (2011) 3113-3124.

[17] S. A. Al-Sanea, M. F. Zedan, S. N. Al-Hussain, Effect of thermal mass on performance of insulated building walls and the concept of energy savings potential, Applied Energy 89 (2012) 430-442.

[18] S. A. Al-Sanea, M. F. Zedan, S. N. Al-Hussain, Effect of masonry material and surface absorptivity on critical thermal mass in insulated building walls, Applied Energy 102 (2013) 1063-1070

[19] M. Ozel, K. Pihtili, Optimum location and distribution of insulation layers on building walls with various orientations, Building and Environment 42 (2007) 3051-3059.

[20] M. Ozel, Effect of insulation location on dynamic heat-transfer characteristics of building external walls and optimization of insulation thickness, Energy and Buildings 72 (2014) 288-295.

[21] D. E. M. Bond, W. W. Clark, M. Kimber, Configuring wall layers for improved insulation performance, Applied Energy 112 (2013) 235-245.

[22] P. Gori, C. Guattari, L. Evangelisti, F. Asdrubali, Design criteria for improving insulation effectiveness of multilayer walls, International Journal of Heat and Mass Transfer 103 (2016) 349-359.

[23] L. Y. Zhang, L. W. Jin, Z. N. Wang, J. Y. Zhang, X. Liu, L. H. Zhang, Effects of wall configuration on building energy performance subject to different climatic zones of China, Applied Energy 185 (2017) 1565-1573

[24] D. I. Kolaitis, E. Malliotakis, D. A. Kontogeorgos, I. Mandilaras, D. I. Katsourinis, M. A. Founti, Comparative assessment of internal and external thermal insulation systems for energy efficient retrofitting of residential buildings, Energy and Buildings 64 (2013) 123-131.

[25] T. Ihara, A. Gustavsen, B. P. Jelle, Effect of facade components on energy efficiency in office buildings, Applied Energy 158 (2015) 422-432.

[26] O. T. Masoso, L. J. Grobler, A new and innovative look at anti-insulation behaviour in building energy consumption, Energy and Buildings 40 (2008) 1889-1894.

[27] Y. M. Idris, M. Mae, Anti-insulation mitigation by altering the envelope layers' configuration, Energy and Buildings 141 (2017) 186-204

[28] X. Meng, T. Luo, Y. Gao, L. Zhang, X. Huang, C. Hou, Q. Shen, E. Long, Comparative analysis on thermal performance of different wall insulation forms under the air-conditioning intermittent operation in summer, Applied Thermal Engineering 130 (2018) 429-438.

[29] T. Pekdogan, T. Basaran, Thermal performance of different exterior wall structures based on wall orientation, Applied Thermal Engineering 122 (2017) 15-24.

[30] M. Ciampi, F. Fantozzi, F. Leccese, G. Tuoni, On the optimization of building envelope thermal performance: Multi-layered wall design to minimize heating and Cooling plant intervention in the case of time varying external temperature fields, Civil Engineering and Environmental Systems 20 (2003) 231-254.

[31] H. S. Carslaw, J. C. Jaeger, Conduction of Heat in Solids, Clarendon Press, Oxford, 1959.

[32] D. Maillet, S. André, J. C. Batsale, A. Degiovanni, C. Moyne, Thermal Quadrupoles: Solving the Heat Equation through Integral Transforms (2000) Wiley, Chichester.

[33] Y. Chen, A. K. Athienitis, K. E. Galal, Frequency domain and finite difference modeling of ventilated concrete slabs and comparison with field measurements: Part 2. Application, International Journal of Heat and Mass Transfer 66 (2013) 957-966.

[34] S. Ginestet, T. Bouache, K. Limam, G. Lindner, Thermal identification of building multilayer walls using reflective Newton algorithm applied to quadrupole modelling, Energy and Buildings 60 (2013) 139-145.

[35] European Standard EN ISO 13786, Thermal performance of building components - Dynamic thermal characteristics - Calculation methods (2008).

[36] P. Gori, L. Evangelisti, C. Guattari, Description of multilayer walls by means of equivalent homogeneous models, International Communications on Heat and Mass Transfer, 91 (2018) 30-39.

[37] D. Mazzeo, G. Oliveti, N. Arcuri, Influence on internal and external boundary conditions on the decrement factor and time lag heat flux of building walls in steady periodic regime, Applied Energy 164 (2016) 509-531.

[38] F. Fantozzi, P. Galbiati, F. Leccese, G. Salvadori, M. Rocca, Thermal analysis of the building envelope of lightweight temporary housing, Journal of Physics: Conference Series 547 (2014) 1-10, Article number 012011.

[39] Kuehn, T.H., Ramsey, J.W., Threlkeld, J.L., Thermal Environmental Engineering (3rd Ed.), Prentice Hall, NJ (USA), 1998.

[40] Z. Tian, X. Zhang, X. Jin, X. Zhou, B. Si, X. Shi, Towards adoption of building energy simulation and optimization for passive building design: A survey and a review, Energy and Buildings 158 (2018) 1306-1316.

[41] M. Ciampi, F. Leccese, G. Tuoni, Building-plant interaction: a parameter to optimize the distribution of thermal resistance and heat capacity in external walls of buildings. IBPC 2003 – Proc. of the 2nd Int. Building Physics Conf.: «Research in Building Physics», Leuven (B), pp. 335-342, 2003.

[42] M. Ciampi, F. Leccese, G. Tuoni, Multi-layered walls design to optimize building-plant interaction, International Journal of Thermal Science 43 (2004) 417-429.

[43] Decreto interministeriale 26 giugno 2015 - Applicazione delle metodologie di calcolo delle prestazioni energetiche e definizione delle prescrizioni e dei requisiti minimi degli edifici, 2015 (in Italian).

[44] European Standard EN 12524, Building Materials And Products - Hygrothermal Properties - Tabulated Design Values (2001).

[45] European Standard EN ISO 10456, Building Materials and Products - Hygrothermal Properties - Tabulated Design Values and Procedures for Determining Declared and Design Thermal Values (2007).

[46] F. Leccese, G. Tuoni, S. Pau, G. Salvadori, Vibro-compressed concrete hollow blocks with high thermal performance: steady-state and transient thermal behavior, CLIMA 2010 – Proc. of the 10th REHVA World Congress, Antalya (TR), ISBN: 978-975-6907-14-6, Vol. cd rom, paper n. R2-TS26-PP05, pp. 1-8, 2010.

[47] I.B. Topcu, B. Isikdag, Manufacture of high heat conductivity resistant clay bricks containing perlite, Building and Environment 42(2007) 3540–3546.

Appendix A-
Lumped capacitance model and optimization of the external walls stratigraphies

A significant problem implied by envelope walls' dynamic thermal behaviour can be stated as centred, on the one hand, on the question of how to define the layer sequence of a wall provided with a thermal resistance R (including surface thermal resistances) and a thermal capacity C fitting for minimizing the dynamic thermal transmittance Y_{ie} (i.e. the decrement factor f_a); on the other hand, on the question of how to define the layer sequence fitting for maximizing the time lag φ.
As a first step, the problem will be solved by considering a lumped-element model. According to this model, the definition "wall stratigraphy" refers to how many purely resistive layers provided with a thermal resistance r_s and how many purely capacitive layers provided with a thermal capacity c_s constitute that specific wall on the basis of a given layer sequence. A *(2n+1)* layered wall, consisting of n capacitive layers and $n+1$ resistive layers, can be outlined as follows [30,42]:

$$[interior]\ [r_n]\ [c_n]\ [r_{n-1}].....[r_1]\ [c_1]\ [r_0]\ [exterior] \qquad \text{(A1)}$$

with $R = \Sigma r_s$ and $C = \Sigma c_s$ (see Figure A1).

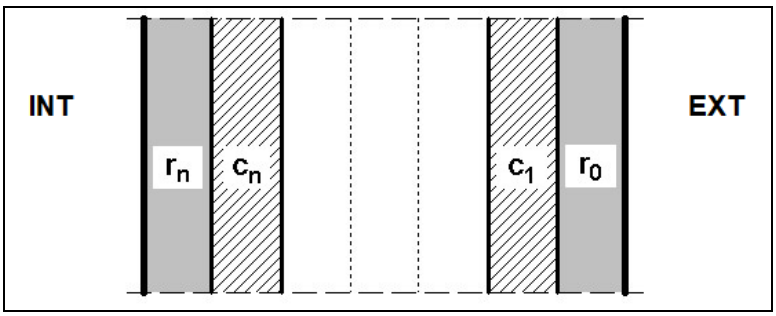

Figure A1- Lumped capacitance model fora an external wall composed of $2n+1$ layers (n capacitive layers and $n+1$ resistive layers).

Given that the different resistive and capacitive layers are respectively represented by triangular matrices of the following type:

$$\begin{pmatrix} 1 & r_s \\ 0 & 1 \end{pmatrix} \quad ; \quad \begin{pmatrix} 1 & 0 \\ j\omega c_s & 1 \end{pmatrix} \qquad \text{(A2)}$$

for $n=\infty$, we obtain a typical homogeneous wall (a wall with uniformly distributed capacity C and thermal resistance R).
The symmetry property shown by the wall transfer matrix element Z_{12} (which we have highlighted and discussed previously) has as a consequence that symmetry is a compulsory requirement for "optimal" layer sequence to be so defined according to the above meaning.
The problem of defining the layer sequence able to minimize Y_{ie} is characterised by the following non-dimensional parameter:

$$\gamma = \omega RC \qquad \text{(A3)}$$

which corresponds to the product of an external thermal field angular frequency ω and the wall's time constant RC.
The obtained results can be summarized as follows [30,42]. For $\gamma < 18$, the optimal symmetry configuration is that obtained with n =1 (three-layered wall), whose capacitive layer (C) is placed between two identical resistive layers ($R/2$), of the following type: *[interior] [R/2] [c] [R/2] [exterior]* (named $\overline{T_1}$). Such a configuration is characterised by $Z_{12} = R\left[1 + j\gamma/4\right]$ from which

$Y_{ie} = 1/R\sqrt{1+\gamma^2/16}$ and $\varphi = (P/2\pi)\arctan(\gamma/4)$ can be derived. For $18 < \gamma < 42$, the optimal symmetry structure is that obtained with n =2 (five-layered wall), of the following type: *[interior] [r_0] [c_1] [r_1] [c_1] [r_0] [exterior]* (named T_2). For $42 < \gamma < 76$ the optimal solution is a *T3* symmetry structure obtained with n =3 (seven-layered wall). For $76 < \gamma < 100$ the optimal solution is a *T4* symmetry structure obtained with n =4 (nine-layered wall), and so on.
For each case with n>1, the optimal resistance and capacity values corresponding to the different layers are dependent on the γ value. It has been proved [30,42] that entirely symmetric walls $\overline{T}_n$, consisting of n capacities and $n+1$ resistances whose values are all identical, with $c_n=C/n$ and $r_n=R/(n+1)$, approximate with a very good accuracy the behaviour of the above defined optimal configurations T_n, within the respective γ intervals. For the sake of simplicity, the following analysis will uniquely include type $\overline{T}_n$ configurations. As a particular example, with regard to configuration $\overline{T}_2$, it can be derived:

$$Z_{12} = R\,[1 + j\,(2/3)(\gamma/3) - (1/12)(\gamma/3)^2] \qquad \text{(A4)}$$

As a second step, it must be observed that whatever real wall can be outlined as a lumped-parameter wall provided with a sufficiently high number of layers. The above presented analysis shows that, for a given γ, the optimal stratigraphy is characterised by a low n value, which excludes the possibility of it being other than a lumped-parameter stratigraphy. The lumped parameter model is therefore not limitative. Even the problem of defining the layer sequence fitting for maximizing the time lag φ is characterised by a dimensional parameter γ; the solution to this problem is very similar to the solution previously obtained with regard to minimizing Y_{ie}, except for the transition from one optimal layer sequence to another takes place for considerably lower γ values. The analysis turns out to be very simple when its spectrum is limited to entirely symmetric type $\overline{T}_n$ walls. If such is the case: for $\gamma < 3.5$, a type $\overline{T}_1$ wall gives an advantageous solution, with n =1 (three-layered wall); for $3.5 < \gamma < 6.7$, a type $\overline{T}_2$ wall gives an advantageous solution, with n =2 (five-layered wall); for $6.7 < \gamma < 10.1$, a type $\overline{T}_3$ wall gives an advantageous solution, with n =3 (seven-layered wall); and so on.
In the case of high γ values, the number of layers which are needed to maximize the time lag φ is found to be in its turn very high, whereas the relevant structure approximates a homogeneous wall's structure, with an uniform distribution of R (including surface thermal resistances) and C.

Example

In the following, the behaviour of lumped-parameter walls, whose structure has been optimized according to the above described theory, will be compared with that of the walls which we have studied previously.
More precisely, for each of the walls *PT*, *P1*, *P2*, *P3*, the corresponding optimal lumped-parameter wall has been considered: Y_{ie} optimized is X_Y, φ optimized is X_φ.
Table A1 shows the performance values of f_a, φ and Y_{ie}, relating to the four walls *PT*, *P1*, *P2* and *P3*, where, for each of them, the corresponding lumped-parameter walls X_Y, and X_φ have been considered. For the sake of comparison, each wall's text box shows also the relevant *SE* layer sequence, along with the equivalent homogeneous layer *SO* (see also Figure 4).
The X_Y lumped-parameter walls, which have been built to minimize Y_{ie}, have turned out to be, on the one hand, five-layered for *P1*, *P2* and *P3*, on the other hand, seven-layered for *PT*. Walls X_φ, which have been built to minimize φ, have turned out to be distinctly more fractionated: depending on wall type, their layer number falls in fact in the range of 15-30.

Stratigraphy	Wall type											
	PT (294 kg/m^2)			**P1** (186 kg/m^2)			**P2** (134 kg/m^2)			**P3** (85 kg/m^2)		
	f_a (-)	φ (h)	Y_{ie} (W/m^{2}K)	f_a (-)	φ (h)	Y_{ie} (W/m^{2}K)	f_a (-)	φ (h)	Y_{ie} (W/m^{2}K)	f_a (-)	φ (h)	Y_{ie} (W/m^{2}K)
SE	0.054	12.3	0.017	0.104	10.3	0.033	0.153	9.27	0.049	0.264	8.34	0.086
SO	0.044	19.4	0.014	0.105	15.4	0.034	0.167	13.1	0.053	0.281	10.6	0.091
X_Y	0.019	14.2	0.006	0.050	12.7	0.016	0.087	11.6	0.028	0.170	10.0	0.055
X_φ	0.0411	19.4	0.013	0.097	15.4	0.031	0.151	13.2	0.048	0.244	10.7	0.079

Table A1- Dynamic thermal properties of the analysed walls.

It must be noted that the φ values, corresponding to X_φ lumped-parameter wall, prove to be conspicuously higher when compared to those pertaining to *SE* layer sequence. The former values approximate very closely to those relating to the equivalent homogeneous layer *SO*, whereas X_Y values are distinctly inferior to those relating to both *SE* and *SO*. If the aim is to evaluate the highest theoretically possible φ values relating to the walls under examination, it is therefore not necessary to take into account extremely fractionated lumped-parameter walls, the reason being that such values coincide with a good accuracy with the values relating to the corresponding homogeneous walls.

Table A1 clearly displays how Y_{ie} shows very low values in relation to X_Y lumped-parameter walls; with regard to each of the walls under examination (*PT*, *P1*, *P2* and *P3*), such values must be considered as the theoretically lowest possible values.

Despite the obvious notion that a perfect equivalent to theoretically conceived lumped-parameter walls is impossible in practical terms, it must be noted that a concrete or limestone layer approximates (and often with an acceptable accuracy) to a purely capacitive layer, whereas a synthetic thermal insulation layer gives an excellent level of approximation to a purely resistive layer. Finally, it must be noted that the current market makes available concrete or clay blocks provided with a multi-layer insulation. Such a solution makes it possible to construct walls approximating how type *X* lumped-parameter walls behave according to the above.